RAREFIED GAS FLOW THROUGH ANNULAR MICROTUBE AT CONSTANT AND EQUAL WALL TEMPERATURES

Iva I. GURANOV [1*], ***Snežana S. MILIĆEV*** [1], ***Nevena D. STEVANOVIĆ*** [1]

[1]University of Belgrade - Faculty of Mechanical Engineering, Kraljice Marije 16, 11120 Belgrade, Serbia

[*] Corresponding author; E-mail: iguranov@mas.bg.ac.rs

The coaxial microtubes, which can be transparent, flexible, and biocompatible, are often part of micro-electro-mechanical systems. This paper examines the steady, subsonic rarefied gas flow through an axisymmetric microtube with an annular cross-section, induced by pressure difference. The flow is considered compressible and non-isothermal, with constant inner and outer wall temperatures. The study uses continuum approach based on continuity, momentum and energy equations together with slip and temperature jump boundary conditions. The perturbation method is used and enables including effects of inertia, convection and expansion work. Hence, analytical solutions for velocity, pressure and temperature are obtained, which allows analysis of all named effects along with annular microtube geometry. These results provide optimizing microtube designs in practical applications. Regarding solutions are analytical, they can be useful as a criterion for validating the accuracy and reliability of numerical solutions of similar problems.

Keywords: *rarefied gas, slip flow, temperature jump, compressible, incompressible, annular microtube*

1. Introduction

With the rapid development of microdevices across industries [1]-[3], understanding heat transfer in microelements is crucial. Micro-heat exchangers are widely used, including in medicine, for cryosurgical probes treating tumors and cardiac arrhythmias. For instance, the Joule-Thomson cryogenic refrigerator, integral to cryosurgical probes, features microtube diameters ranging from tens to hundreds of microns. These devices offer simplicity and compactness, enhancing their applicability [4].

Micro-annuli are key micro-geometries in micro-fluidic systems, applicable from basic heat exchangers to complex nuclear reactors [5]. Coaxial tube configuration is present in variuos technological applications including pressure measuring in vacuum gadgets [6], multilayer insulation blankets used in micro heat exchangers, cryogenic systems and space vehicles [7]. Consequently, understanding non-isothermal gas flow in annular microtubes under various temperatures is crucial for many devices, necessitating a thorough understanding of flow characteristics.

Corresponding works with non-isothermal coaxial microtubes are limited. These problems are mostly investigated numerically. Maharjan et al. [8], Pantazis et al. [9] and Sharipov and Bertoldo [10] explored heat transfer in the axial flow of rarefied gas between coaxial cylinders maintained at

different temperatures. Maharjan et al. [8] based research on the S-model kinetic equation, DSMC technique and CFD with Lin and Willis boundary condition [8], while Pantazis et al. [9] employed kinetic S-model with Cercignani-Lampis boundary condition. Aoki et al. investigated rarefied gas flow between coaxial elliptical cylinders with different uniform temperatures on the basis of kinetic theory [11]. Char and Tai [12] examined laminar incompressible rarefied gas flow in a micro-annulus with constant wall temperatures.

Several researchers obtained analytical results for the flow of rarefied gas through microtubes. Weng and Chen [13] analyzed natural convection in vertical annular microtube gas flow with constant inner wall temperature. Shamshiri et al. [14] modeled transport mechanisms in rarefied gas flow in the slip regime between a shaft and its cylindrical housing, using incompressible Navier-Stokes-Fourier equations. Duan and Muzychka [15] studied heat transfer in rarefied incompressible gas flow through an annular microtube, considering cases with both walls conducting heat and one wall being adiabatically insulated. Barbera and Brini [16] explored steady-state heat transfer between two coaxial cylinders at different temperatures by 13 moment equations, where the inner cylinder moves in the axial direction.

None of the introduced literature, to the authors' knowledge, has dealt with the pressure driven compressible rarefied gas flows in annular microtubes, with constant and equal wall temperatures. Therefore, this paper examines rarefied pressure driven non-isothermal steady compressible subsonic gas flow through an axisymmetric annular microtube. Besides, the contribution of the solution presented in this paper is in analytical approach. Obtained analytical solutions are easily applicable, repeatable and can serve as a reference for numerical solutions of similar problems.

2. Problem description and governing equations

The annular microtube has a constant cross-section (fig. 1). The temperatures of the inner and outer walls are constant, equal to each other, and denoted by $\tilde{T}_w$ (dimensional quantities are indicated with tilde).

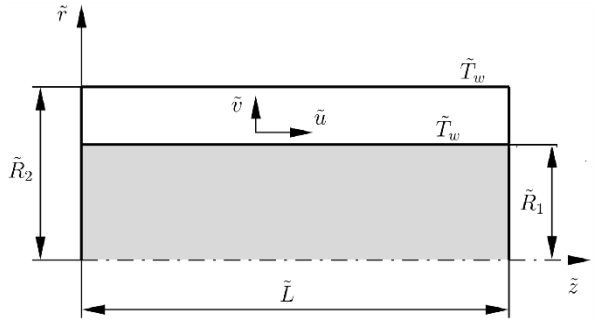

Figure 1: Annular microtube geometry.

For the stationary axisymmetric compressible non-isothermal flow the system of equations comprises of the continuity equation, the momentum equations in the axial and radial directions, the energy equation in the differential form [17]. When studying compressible gas flow, the equations must incorporate an equation of state for an ideal gas [17].

Maxwell developed the slip boundary condition for velocity using kinetic theory of monatomic gases [18]:

$$\tilde{u} - \tilde{u}_w = -\frac{2-\sigma_v}{\sigma_v}\tilde{\lambda}\frac{\partial \tilde{u}}{\partial \tilde{r}}|_w + \frac{3}{4}\frac{\tilde{\mu}}{\tilde{\rho}\,\tilde{T}}\frac{\partial \tilde{T}}{\partial \tilde{z}}|_w, \quad \tilde{v} = \tilde{v}_w. \tag{1}$$

The boundary condition for the temperature field, was derived by Smoluchowski [19], also using the kinetic theory of gases. For flows in tubes, Smoluchowski boundary condition can be written as:

$$\tilde{T} - \tilde{T}_w = -\frac{2-\sigma_T}{\sigma_T}\frac{2\kappa}{\kappa+1}\frac{\tilde{\lambda}}{\mathrm{Pr}}\frac{\partial \tilde{T}}{\partial \tilde{r}}|_w. \tag{2}$$

3. Solution procedure

To convert dimensional equations into dimensionless form, it is necessary to introduce appropriate reference quantities. As the values of the Knudsen and Mach numbers increase from the inlet to the outlet of the tube, choosing the outlet cross-section as the reference ensures that the entire tube will have a subsonic flow regime under slip conditions, if that condition is met at the outlet. The dimensionless quantities are:

$$u = \frac{\tilde{u}}{\tilde{u}_r}, \quad v = \frac{\tilde{v}}{\tilde{u}_r}, \quad p = \frac{\tilde{p}}{\tilde{p}_r}, \quad \rho = \frac{\tilde{\rho}}{\tilde{\rho}_r}, \quad T = \frac{\tilde{T}}{\tilde{T}_w}, \quad r = \frac{\tilde{r}}{\tilde{R}_r}, \quad z = \frac{\tilde{z}}{\tilde{L}}, \quad \mu = \frac{\tilde{\mu}}{\tilde{\mu}_r}, \quad k = \frac{\tilde{k}}{\tilde{k}_r}.$$

According to the molecular model of hard spheres, the dimensionless thermal conductivity k and dynamic viscosity μ follow $k = \mu = T^a$. The solutions are based on the following flow conditions assumptions:

- the reference diameter of the tube is much smaller than the length of the tube, so it is possible to introduce a small parameter $\varepsilon = 2\left(\tilde{R}_2 - \tilde{R}_1\right)/\tilde{L}, \varepsilon \ll 1$;
- due to the constant cross-section of the annular microtube, it is assumed that the radial velocity component is much smaller than the longitudinal component $\tilde{v} = \varepsilon\tilde{V}, \tilde{V} = \mathcal{O}(1)$;
- for subsonic flow with slip, the values of the reference Mach and reference Knudsen numbers are small and can it be assumed $\kappa \mathrm{Ma_r}^2 = \gamma\varepsilon^m, \gamma = \mathcal{O}(1), m > 0$ and $\mathrm{Kn_r} = \eta\varepsilon^n, \eta = \mathcal{O}(1), n > 0$;
- the subsonic condition also permits the assumption regarding the order of magnitude of the ratio of the square of the reference Mach number to the reference Reynolds number $\kappa \mathrm{Ma_r}^2/\mathrm{Re_r} = \beta\varepsilon, \beta = \mathcal{O}(1)$.

The reference Mach, Knudsen, Reynolds and Prandtl numbers are defined as follows:

$$\mathrm{Ma_r} = \frac{\tilde{u}_r}{\sqrt{\kappa\tilde{p}_r/\tilde{\rho}_r}}, \quad \mathrm{Kn_r} = \frac{\tilde{\lambda}_r}{2(\tilde{R}_2 - \tilde{R}_1)}, \quad \mathrm{Re_r} = \frac{2\tilde{\rho}_r\tilde{u}_r(\tilde{R}_2 - \tilde{R}_1)}{\tilde{\mu}_r}, \quad \mathrm{Pr} = \mathrm{Pr_r} = \tilde{c}_p\frac{\tilde{\mu}_r}{\tilde{k}_r}. \tag{3}$$

From the definition of reference Mach, Reynolds and Knudsen number, eq. (3), the relation between them is:

$$\mathrm{Kn_r} = \sqrt{\frac{\pi\kappa}{2}}\frac{\mathrm{Ma_r}}{\mathrm{Re_r}}. \tag{4}$$

From assumptions about Mach number follows the connection between the Reynolds number and the small parameter ε:

$$\mathrm{Re_r} = \gamma\varepsilon^{m-1}/\beta, \tag{5}$$

where the positive exponent value for the small parameter ε ($m > 1$) indicates low Reynolds number flow, while negative exponents ($m \leqslant 1$) correspond to high Reynolds numbers. The relationship between parameters γ, η, and β is derived from assumptions regarding Mach, Knudsen, Reynolds numbers and eq. (4), eq. (5): $\gamma = \beta^2\pi/2\eta^2$. Also, the parameters m and n are not independent. The dependence between them follows from the assumptions and the expression (4):

$$2n + m = 2. \tag{6}$$

With the already stated $m > 0$ and $n > 0$, from the relation (6), the domain of these parameters is $n \in (0,1)$ and $m \in (0,2)$. For flows at low Reynolds numbers ($\mathrm{Re_r} < 1$) $m > 1$, the domain of parameters is:

$$1 < m < 2, \quad 0 < n < 1/2. \tag{7}$$

For flows at moderately high Reynolds numbers ($\mathrm{Re_r} \geqslant 1$), when $m \leqslant 1$, the parameters m and n are:

$$0 < m \leqslant 1, \quad 1/2 \leqslant n < 1. \tag{8}$$

The continuity equation, momentum equations for the axial and radial directions and energy equation are transformed into dimensionless form:

$$\frac{2}{r}\frac{\partial(r\rho V)}{\partial r} + \frac{\partial(\rho u)}{\partial z} = 0, \tag{9}$$

$$\gamma\varepsilon^m\rho\left(2V\frac{\partial u}{\partial r} + u\frac{\partial u}{\partial z}\right) = -\frac{\partial p}{\partial z} + \frac{4\beta}{r}\frac{\partial}{\partial r}\left(\mu r\frac{\partial u}{\partial r}\right), \tag{10}$$

$$\frac{\partial p}{\partial r} = 0, \tag{11}$$

$$\mathrm{Pr}\frac{\gamma\varepsilon^m}{4\beta}\rho\left(2V\frac{\partial T}{\partial r} + u\frac{\partial T}{\partial z}\right) = \frac{1}{r}\frac{\partial}{\partial r}\left(kr\frac{\partial T}{\partial r}\right) + \mathrm{Pr}\frac{\kappa-1}{\kappa}\gamma\varepsilon^m\left[\frac{u}{4\beta}\frac{\partial p}{\partial z} + \mu\left(\frac{\partial u}{\partial r}\right)^2\right]. \tag{12}$$

The pressure does not depend on the radial coordinate r, eq. (11). Considering that the flow is axisymmetric, it is concluded that the pressure depends only on the longitudinal coordinate z, so $\partial p/\partial z = \mathrm{d}p/\mathrm{d}z = p'$. The dimensionless form of the equation of state of an ideal gas should be added to the dimensionless system of equations (9)-(12):

$$p = \rho T. \tag{13}$$

From the boundary condition for velocity in the dimensional form, expression (1), it follows that dimensionless boundary condition for the inner and outer walls of the tube is:

$$u|_{r=R_1} = \frac{2-\sigma_v}{\sigma_v}2\mathrm{Kn_r}\frac{T^{a+0,5}}{p}\frac{\partial u}{\partial r}|_{r=R_1}, \quad u|_{r=R_2} = -\frac{2-\sigma_v}{\sigma_v}2\mathrm{Kn_r}\frac{T^{a+0,5}}{p}\frac{\partial u}{\partial r}|_{r=R_2}. \tag{14}$$

Starting from the dimensional form of Smoluchowski boundary condition eq. (2), the dimensionless form for the inner and outer walls of the microtube is:

$$T|_{r=R_1} = 1 - \frac{2-\sigma_T}{\sigma_T}\frac{4\kappa}{\kappa+1}\frac{\mathrm{Kn_r}}{\mathrm{Pr}}\frac{T^{a+0,5}}{p}\frac{\partial T}{\partial r}|_{r=R_1}, T|_{r=R_2} = 1 + \frac{2-\sigma_T}{\sigma_T}\frac{4\kappa}{\kappa+1}\frac{\mathrm{Kn_r}}{\mathrm{Pr}}\frac{T^{a+0,5}}{p}\frac{\partial T}{\partial r}|_{r=R_2}. \tag{15}$$

To solve the system of equations (9)-(13) with boundary conditions (14), (15) the perturbation approach is applied. All quantities are expressed in the form of a perturbation series, with two approximations each $f = f_0 + \mathrm{Kn_r}f_1 + \mathcal{O}(\mathrm{Kn_r^2})$. With the intention that all effects occur in the second approximation, from expressions (10), (12), (6) it follows for the parameters m and n it is only possible $m = n = 2/3$. Therefore, from the equation (8) this case corresponds to moderately high Reynolds numbers.

By incorporating all quantities, whose solution needs to be achieved, in the form of a perturbation series, into the system of equations in dimensionless form, two systems are obtained:

$$\varepsilon^0\colon \int_{R_1}^{R_2} 2\rho_0 u_0 r\,\mathrm{d}r = \dot{m}_0, \tag{16}$$

$$p_0{}' = \frac{4\beta}{r}\frac{\partial}{\partial r}\left(T_0^a r\frac{\partial u_0}{\partial r}\right), \tag{17}$$

$$0 = \frac{1}{r}\frac{\partial}{\partial r}\left(rT_0^a\frac{\partial T_0}{\partial r}\right), \tag{18}$$

$$u_0|_{r=R_1} = 0, \quad u_0|_{r=R_2} = 0, \tag{19}$$

$$T_0|_{r=R_1} = 1, \quad T_0|_{r=R_2} = 1, \tag{20}$$

$$\varepsilon^n\colon \int_{R_1}^{R_2} 2(\rho_0 u_1 + \rho_1 u_0) r \mathrm{d}r = \dot{m}_1, \tag{21}$$

$$\frac{\gamma}{\eta}\rho_0\left(2V_0\frac{\partial u_0}{\partial r} + u_0\frac{\partial u_0}{\partial z}\right) + {p_1}' = \frac{4\beta}{r}\frac{\partial}{\partial r}\left[rT_0^a\left(\frac{\partial u_1}{\partial r} + a\frac{T_1}{T_0}\frac{\partial u_0}{\partial r}\right)\right], \tag{22}$$

$$\frac{\mathrm{Pr}}{4}\frac{\gamma}{\beta}\rho_0\left(2V_0\frac{\partial T_0}{\partial r} + u_0\frac{\partial T_0}{\partial z}\right) = \eta\frac{1}{r}\frac{\partial}{\partial r}\left[r\left(\frac{\partial}{\partial r}(T_0^a T_1)\right)\right] + \mathrm{Pr}\gamma\frac{\kappa-1}{\kappa}\left[\frac{u_0}{4\beta}{p_0}' + T_0^a\left(\frac{\partial u_0}{\partial r}\right)^2\right], \tag{23}$$

$$u_1|_{r=R_1} = \frac{2-\sigma_v}{\sigma_v}2\frac{T_0^{a+0,5}}{p_0}\frac{\partial u_0}{\partial r}|_{r=R_1}, \quad u_1|_{r=R_2} = -\frac{2-\sigma_v}{\sigma_v}2\frac{T_0^{a+0,5}}{p_0}\frac{\partial u_0}{\partial r}|_{r=R_2}, \tag{24}$$

$$T_1|_{r=R_1} = -\frac{2-\sigma_T}{\sigma_T}\frac{4\kappa}{\kappa+1}\frac{1}{\mathrm{Pr}}\frac{T_0^{a+0,5}}{p_0}\frac{\partial T_0}{\partial r}|_{r=R_1}, T_1|_{r=R_2} = \frac{2-\sigma_T}{\sigma_T}\frac{4\kappa}{\kappa+1}\frac{1}{\mathrm{Pr}}\frac{T_0^{a+0,5}}{p_0}\frac{\partial T_0}{\partial r}|_{r=R_2}. \tag{25}$$

Solutions are obtained for the known mass flow rate value, which is included in the first approximation: $\dot{m}_0 = R_1 + R_2,\ \dot{m}_1 = 0$. The solution process begins with the energy equation for the first approximation (18) and the boundary conditions for gas temperature on the inner and outer walls eq. (20), providing the first approximation of temperature. Next, the momentum equation in the z direction is solved for the first approximation (17) with velocity boundary conditions eq. (19). Then pressure field for the first approximation is determined using the integral form of the continuity equation (16), with boundary condition for pressure at the outlet cross-section $p_0|_{z=1} = 1$ (the pressure is fully contained in the first approximation). The same procedure applies to the second approximation. The temperature is obtained from the energy equation (23) and the corresponding boundary condition (25), after that the velocity from the momentum equation (22) and velocity boundary condition (24). Finally, the second approximation for the pressure is obtained based on the integral form of the continuity equation (21), where boundary condition for pressure at the exit is $p_1|_{z=1} = 0$.

In view of this, the solutions for the velocity and temperature fields follow:

$$u = u_0 + \mathrm{Kn_r}u_1 = \frac{{p_0}'}{\beta}C_1(r) + \frac{\mathrm{Kn_r}}{\beta}\left\{{p_1}'C_1(r) + \frac{2-\sigma_v}{\sigma_v}\frac{{p_0}'}{p_0}C_2(r) + \right.$$
$$+\mathrm{Kn_r}\mathrm{Re_r^2}{p_0}'\left[73728\pi\beta^2\left(\ln\frac{R_2}{R_1}\right)^3\right]^{-1}\left[\rho_0{p_0}''C_3(r) - \right.$$
$$a\,{p'}_0^2\mathrm{Pr}(\kappa - \left.\left. 1)\left(2\kappa\ln\frac{R_2}{R_1}\right)^{-1}C_5(r)\right]\right\}, \tag{26}$$

$$T = T_0 + \mathrm{Kn_r}T_1 = 1 + \mathrm{Kn_r^2}\mathrm{Re_r^2}\mathrm{Pr}\frac{\kappa-1}{\kappa\beta^2\pi}{p'}_0^2 C_4(r), \tag{27}$$

where functions $C_1(r)$, $C_2(r)$, $C_3(r)$, $C_4(r)$, $C_5(r)$ are given in Appendix.

The pressure field is considered for both compressible flow and when compressibility is neglected.

3.1. The solutions for compressible gas flow

Using the obtained temperature solution eq. (27) and the ideal gas equation of state (13), the density in the first and second approximations is $\rho_0 = p_0$ and $\rho_1 = p_1 - p_0 T_1$. Including the density value into the integral form of the continuity equation (16), (21), the pressure solution for compressible non-isothermal flow of rarefied gas through an annular microtube at moderately high Reynolds numbers is obtained:

$$p = p_0 + \mathrm{Kn_r}p_1 = p_0 + \mathrm{Kn_r}\left[\frac{2-\sigma_v}{\sigma_v}\left(1 - \frac{1}{p_0}\right)C_2C_3 + \right.$$

$$+\mathrm{Kn_r Re_r^2} C_2^3 \left(\ln\frac{R_2}{R_1}\right)^{-4} (6\pi p_0(R_1+R_2))^{-1} \left(C_4 + \mathrm{Pr}\frac{\kappa-1}{\kappa}(a+1)C_5\right)\ln p_0\Big], \quad (28)$$

where pressure in the first approximation is $p_0 = \sqrt{1+64\beta(z-1)C_2}$ and constants C_2, C_3, C_4, C_5 are stated in Appendix.

Based on the general solution for the velocity eq. (26), temperature eq. (27) and the obtained pressure field for compressible flow eq. (28), the velocity and temperature for compressible non-isothermal flow at moderately high Reynolds numbers are:

$$u = u_0 + \mathrm{Kn_r} u_1 = \frac{p_0^2-1}{2p_0\beta(z-1)} C_1(r) + \frac{\mathrm{Kn_r}}{\beta}\Big[\frac{2-\sigma_v}{\sigma_v}\frac{p_0^2-1}{2p_0^2(z-1)} C_2(r) +$$
$$+\frac{16\beta C_2^2 C_1(r)}{3p_0^3}\left(6C_3\frac{2-\sigma_v}{\sigma_v} - \frac{\mathrm{Kn_r Re_r^2} C_2^2(\ln p_0-1)}{\pi(R_1+R_2)}\left(\ln\frac{R_2}{R_1}\right)^{-4}\left(C_4 + \mathrm{Pr}\frac{\kappa-1}{\kappa}(a+1)C_5\right)\right) -$$
$$\frac{\mathrm{Kn_r Re_r^2}(p_0^2-1)^3}{147456\pi p_0^3(z-1)^3\beta^2}\left(\ln\frac{R_2}{R_1}\right)^{-3}\left(\frac{C_3(r)}{4} + \frac{a\,\mathrm{Pr}(\kappa-1)}{8\kappa}\left(\ln\frac{R_2}{R_1}\right)^{-1} C_5(r)\right)\Big], \quad (29)$$

$$T = T_0 + \mathrm{Kn_r} T_1 = 1 + \mathrm{Kn_r^2 Re_r^2 Pr}\frac{\kappa-1}{4\kappa\beta^2\pi}\left(\frac{p_0^2-1}{p_0(z-1)}\right)^2 C_4(r). \quad (30)$$

3.2. The solutions for incompressible gas flow

As results in the literature are given for incompressible flow, solutions were also obtained for the case when compressibility is neglected. For constant density, the density is contained in the first approximation: $\rho_0 = 1$, $\rho_1 = 0$. The assumption of neglected compressibility can be confirmed by small values of the Mach number. Involving density values in the continuity equations in integral form (16), (21), the pressure for non-isothermal flow of rarefied gas through an annular microtube at moderately high Reynolds numbers, when compressibility is neglected is:

$$p = p_0 + \mathrm{Kn_r} p_1 = p_0 + \mathrm{Kn_r}\Big[\frac{2-\sigma_v}{\sigma_v} C_2 C_3 \ln p_0 + \frac{a\mathrm{Kn_r Re_r^2 Pr}}{\kappa\pi}(\kappa-1)C_5 C_6(p_0-1)\Big], \quad (31)$$

where pressure in the first approximation is $p_0 = 1 + 32\beta(z-1)C_2$ and constants C_2, C_3, C_5, C_6 are stated in Appendix.

From the solutions for velocity eq. (26), temperature eq. (27) and pressure eq. (31) follows the temperature and velocity for incompressible non-isothermal flow at moderately high Reynolds numbers:

$$u = u_0 + \mathrm{Kn_r} u_1 = \frac{p_0-1}{(z-1)\beta} C_1(r) + \frac{\mathrm{Kn_r}}{\beta}\Big[\frac{2-\sigma_v}{\sigma_v}\frac{p_0-1}{(z-1)p_0} C_2(r) + 32\beta C_2 C_1(r)\Big(\frac{2-\sigma_v}{\sigma_v}\frac{C_2 C_3}{p_0} +$$
$$+\frac{a\mathrm{Kn_r Re_r^2 Pr}}{\kappa\pi}(\kappa-1)C_5 C_6\Big) - \frac{a\mathrm{Kn_r Re_r^2 Pr}(\kappa-1)}{147456\pi\beta^2\kappa}\left(\ln\frac{R_2}{R_1}\right)^{-4}\left(\frac{p_0-1}{z-1}\right)^3 C_5(r)\Big], \quad (32)$$

$$T = T_0 + \mathrm{Kn_r} T_1 = 1 + \mathrm{Kn_r^2 Re_r^2 Pr}\frac{\kappa-1}{\kappa\beta^2\pi}\left(\frac{p_0-1}{z-1}\right)^2 C_4(r). \quad (33)$$

4. Results

Fig. 2 and fig. 3 show pressure distribution along the microtube and the results for velocity and temperature in three cross-sections. Two gap geometries were chosen to display the results: $R_2/R_1 = 5$ and $R_2/R_1 = 5/3$. The accommodation coefficient for diffuse reflection $\sigma_v = 1$ and ideal energy exchange between the gas and the wall $\sigma_T = 1$ was used, both for the inner and outer walls. In order to compare with the results from the literature, obtained for a diatomic gas, the Prantl number $\mathrm{Pr} = 0.7$ and the heat capacity ratio $\kappa = 7/5$ were chosen.

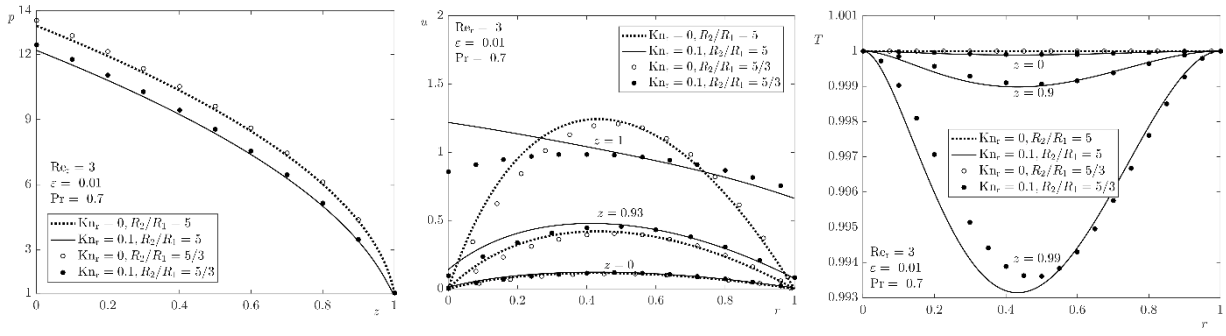

a) b) c)

Figure 2: Results for compressible flow: a) pressure for continuum ($\mathbf{Kn_r = 0}$) and slip ($\mathbf{Kn_r}$ =0.1) eq. (28); b) velocity for continuum (Kn_r=0) and slip (Kn_r=0.1) eq. (29); c) temperature for continuum (Kn_r=0) and slip (Kn_r=0.1) eq. (30).

Fig. 2 shows the results for compressible flow. Fig. 2 a) shows that rarefaction decreases pressure compared to the case when rarefaction is neglected, at the same mass flow rate. Increasing ratio R_2/R_1 leads to the lower pressure along the microtube. Fig. 2 b) shows velocity profiles at three cross-sections. The slip effect on the microtube walls increases from inlet to outlet of the tube. A higher outer-to-inner radius ratio increases velocity profile asymmetry, especially at the outlet. The influence of the R_2/R_1 ratio on the velocity field for non-isothermal compressible flow in an annular microtube is consistent with findings of Taheri and Struchtrup [20] and Taheri et al. [21]. Although non-isothermality exists, for compressible flow at high Reynolds numbers, in the continuum case the temperature profile is constant (fig. 2 c)). The gas temperature at the wall is equal to the wall temperature along the tube, indicating the temperature jump boundary condition did not come to the fore. Increasing the outer-to-inner radius ratio causes greater asymmetry in the temperature profile.

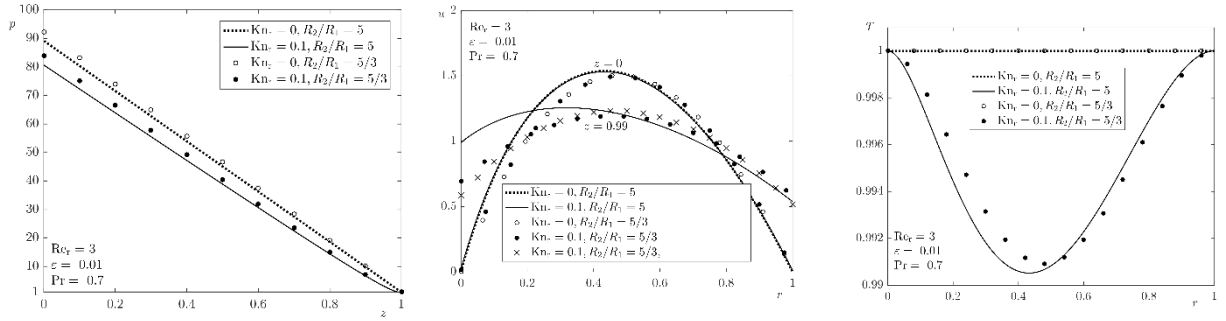

a) b) c)

Figure 3: Results for incompressible flow: a) pressure for continuum ($\mathbf{Kn_r = 0}$) and slip ($\mathbf{Kn_r = 0.1}$) eq. (31), b) velocity for continuum ($\mathbf{Kn_r = 0}$) and slip ($\mathbf{Kn_r = 0.1}$) eq. (32); c) temperature for continuum ($\mathbf{Kn_r = 0}$) and slip ($\mathbf{Kn_r = 0.1}$) eq. (33).

Fig. 3 shows the results for incompressible flow at high Reynolds numbers. For incompressible flow in the continuum case, pressure distribution is linear, but rarefaction lowers pressure along the tube (fig. 3 a)), similar as in [22] and [23]. Increasing the R_2/R_1 ratio pressure decreases, as for compressible flow, especially at higher Knudsen numbers ($\mathrm{Kn_r} = 0.1$). In non-isothermal flow at moderately high Reynolds numbers without considering compressibility, the velocity profile remains unchanged along the microtube in the continuum case (fig. 3 b)). This is due to the linear pressure

distribution in the longitudinal direction. However, considering rarefaction, inertia, convection, expansion work, and viscosity, the velocity profile decreases from the inlet to the outlet of the pipe in the area at half the distance between the inner and outer cylinder of the tube. Conversely, on the walls, slip velocity increases from entrance to exit. Fig. 3 b) also demonstrates the impact of the R_2/R_1 ratio on the velocity field, increasing asymmetry notably at the exit cross-section. This influence mirrors that of compressible flow, as in Taheri and Strachtrap [20] and Taheri et al. [21]. Fig. 3 b) also shows a comparison with the results of Char and Tai [12] and it shows good agreement for the same flow conditions. Fig. 3 c) shows the temperature profile for incompressible flow at high Reynolds numbers. In the continuum case, the temperature is constant, but it varies across the cross-section when rarefaction is considered. Since the density is assumed to be constant, there's no temperature change along the tube. The temperature jump boundary condition, as for compressible flow, did not come to the fore. Increasing the R_2/R_1 ratio lowers the temperature and increases profile asymmetry, similar to the compressible flow case.

5. Conclusion

The increasing prevalence and wide application of micro-electro-mechanical systems, which frequently utilize microtubes, motivates the study of rarefied gas flow. Hence, exploring gas flow in microtubes with various geometries and temperature conditions is highly significant.

This study examines the compressible non-isothermal steady subsonic rarefied gas flow through an axisymmetric microtube with an annular cross-section, driven by a pressure difference between the tube's inlet and outlet. The analysis includes the continuity, momentum and energy equations, with velocity slip and temperature jump boundary conditions. Solutions are derived using a perturbation approach. Using the perturbation method, all quantities are shown with two approximations of the perturbation series. Two approximations include elements of the order of unity and the order of Knudsen's number. The boundary condition of the temperature jump did not come to the fore in the first two approximations of the perturbation series. That is, this effect is smaller than the effects covered by the obtained solution, so the importance of this solution is not diminished.

The increase of outer-to-inner radius ratio causes greater asymmetry of temperature and velocity profile along the microtube. These findings align with existing literature on rarefied gas flows, which confirms accuracy of the solution. Obtained results enhancing understanding of heat transfer in micro-fluidic systems.

Acknowledgment

The results presented here are the result of the research supported by the Ministry of Science, Technological Development and Innovation, Republic of Serbia, Grant No. 451-03-65/2024-03/200105 (2024).

Nomenclature

~	mark above the letter for dimensional sizes
without ~	mark for dimensionless quantities

a	temperature-viscosity parameter [-]
$\beta, \eta, \gamma, m, n$	parameter [-]
c_p	specific heat capacity at constant pressure [$\mathrm{Jkg^{-1}K^{-1}}$]
ε	small parameter [-]
k	thermal conductivity of gas [$\mathrm{Wm^{-1}K^{-1}}$]
κ	the ratio of specific heat capacities [-]
Kn	Knudsen number [-]
λ	the length of the free path of the molecule [m]
L	microtube length [m]
$\dot{m}$	mass flow [$\mathrm{kgs^{-1}}$]
Ma	Mach number [-]
μ	dynamic gas viscosity [Pas]
ν	kinematic gas viscosity [$\mathrm{m^2s}$]
p	pressure [Pa]
Pr	Prandtl number [-]
r, θ, z	coordinates of the cylindrical coordinate system
R_1	inner microtube radius [m]
R_2	outer microtube radius [m]
Re	Reynolds number [-]
ρ	gas density [$\mathrm{kgm^{-3}}$]
σ_T	thermal accommodation coefficient [-]
σ_v	accommodation coefficient of the momentum vector [-]
T	temperature [K]
u	component of the velocity in the longitudinal direction [$\mathrm{ms^{-1}}$]
v, V	radial velocity component [$\mathrm{ms^{-1}}$]
subscript i	inlet cross-section
subscript e	outlet cross-section
subscript r	reference cross-section
subscript w	wall
subscript $0, 1$	first and second approximation

References

[1] Rachkovskij, D. A., *et al.*, Heat Exchange in Short Microtubes and Micro Heat Exchangers with Low Hydraulic Losses, *Microsystem Technologies*, 4 (1998), 3, pp. 151-158

[2] David Doty, F., *et al.*, 1991, The Microtube Strip Heat Exchanger, *Heat Transfer Engineering*, 12 (1991), 3, pp. 31-41

[3] Han, Y., *et al.*, A Review of Development of Micro-Channel Heat Exchanger Applied in Air-Conditioning System, *Energy Procedia*, 14 (2012), pp. 148-153

[4] Ohadi, M., *et al.*, *Next Generation Microchannel Heat Exchangers*, SpringerBriefs in Thermal Engineering and Applied Science, Springer, 2013

[5] Hong, C., *et al*., Friction Factor Correlations of Gas Slip Flow in Concentric Micro Annular Tubes, *Proceedings*, ASME 5th ICNMM, Puebla, Mexico, 2007, ICNMM2007-30064, pp. 365-372

[6] Jitschin, W., Ludwig, S., Dynamical behavior of the Pirani sensor, *Vacuum*, 75 (2004), pp. 169–176

[7] Sun, P. J., *et al*., Experimental study of the influences of degraded vacuum on multilayer insulation blankets, *Cryogenics*, 49 (2009), pp. 719-726

[8] Maharjan, D., *et al*., Simulation of Heat Transfer Across Rarefied Gas in Annular and Planar Geometries: Comparison of Navier-Stokes, S-Model and DSMC Methods Results, *Proceedings*, ASME 13th ICNMM, San Francisco, CA, 2015, ICNMM2015-48034, V001T04A032, pp. 1-10

[9] Pantazis, S., Valougeorgis, D., Heat Transfer Through Rarefied Gases Between Coaxial Cylindrical Surfaces with Arbitrary Temperature Difference, *European Journal of Mechanics - B/Fluids*, 29 (2010), 2, pp. 494-509

[10] Sharipov, F., Bertoldo, G., Heat transfer through a rarefied gas confined between two coaxial cylinders with high radius ratio, *Journal of Vacuum Science & Technology*, 24 (2006), 6, pp. 2087–2093

[11] Aoki, K., *et al*., A Rarefied Gas Flow Induced by a Temperature Field: Numerical Analysis of the Flow between Two Coaxial Elliptic Cylinders with Different Uniform Temperatures, *Computers & Mathematics with Applications*, 35 (1998), 1/2, pp. 15-28

[12] Char, M. I., Tai, B. C., Effects of Viscous Dissipation on Slip-Flow Heat Transfer in a Micro Annulus, *International Journal of Heat and Mass Transfer*, 53 (2010), 7-8, pp. 1402-1408

[13] Weng, H. C., Chen, C. K., Drag Reduction and Heat Transfer Enhancement Over a Heated Wall of a Vertical Annular Microchannel, *International Journal of Heat and Mass Transfer*, 52 (2009), 3-4, pp. 1075-1079

[14] Shamshiri, M., *et al*., Investigation of Flow and Heat Transfer Characteristics of Rarefied Gaseous Slip Flow in Nonplanar Micro-Couette Configuration, *International Journal of Thermal Sciences*, 54 (2012), pp. 262-275

[15] Duan, Z., Muzychka, Y. S., Slip Flow Heat Transfer in Annular Microchannels With Constant Heat Flux, *Journal of Heat Transfer*, 130 (2008), 9, pp. 092401-1-8

[16] Barbera, E., Brini, F., Non-isothermal axial flow of a rarefied gas between two coaxial cylinders, *Atti della Accademia Peloritana dei Pericolanti - Classe di Scienze Fisiche, Matematiche e Naturali*, 95 (2017), 2, pp. A1-1-12

[17] Guranov, I., Strujanja razre enog gasa u mikrocevima (Rarefied gas flow in microtubes), (in Serbian language), Ph.D. thesis, University of Belgrade - Faculty of Mechanical engineering, Belgrade, Serbia, 2023

[18] Maxwell, J. C., On stresses in rarefied gases arising from inequalities of temperature, *Philosophical Transactions of the Royal Society of London*, 170 (1879), pp. 231-256

[19] Smoluchowski von Smolan, R. M., Ueber Warmeleitung in verdunnten Gasen, *Annals of Physics*, 300 (1898), pp. 101-130

[20] Taheri, P., Struchtrup, H., Poiseuille Flow of Moderately Rarefied Gases in Annular Channels, *International Journal of Heat and Mass Transfer*, 55 (2012), 4, pp. 1291-1303

[21] Taheri, P., *et al*., Couette and Poiseuille Microflows: Analytical Solutions for Regularized 13-moment Equations, *Physics of Fluids*, 21 (2009), pp. 017102-1-11

[22] Guranov, I., *et al*., Non-isothermal Rarefied Gas Flow in Microtube with Constant Wall Temperature, *Advances in Mechanical Engineering*, 13 (2021), 11, pp. 1-9

[23] Asako, Y., Hong, C., On Temperature Jump Condition for Slip Flow in a Micro-channel with Constant Wall Temperature, *International Journal of Thermal Sciences*, 139 (2007), p. 072402

Appendix

$$C_1 = R_1^2 - R_2^2, \tag{34}$$

$$C_2 = \ln\frac{R_2}{R_1}\left[(R_1 - R_2)\left(C_1 + (R_1^2 + R_2^2)\ln\frac{R_2}{R_1}\right)\right]^{-1}, \tag{35}$$

$$C_3 = 2\left[C_1^2 + 4R_1R_2\left(C_1 + (R_1^2 - R_1R_2 + R_2^2)\ln\frac{R_2}{R_1}\right)\ln\frac{R_2}{R_1}\right]\left[R_1R_2\left(\ln\frac{R_2}{R_1}\right)^2\right]^{-1}, \tag{36}$$

$$C_4 = \left[36C_1^4 + 63C_1^3(R_1^2 + R_2^2)\ln\frac{R_2}{R_1} + 44(R_1^8 - R_1^6R_2^2 - R_1^2R_2^6 + R_2^8)\left(\ln\frac{R_2}{R_1}\right)^2 + \right.$$
$$\left. + 12(R_1^8 - R_2^8)\left(\ln\frac{R_2}{R_1}\right)^3\right]2\ln\frac{R_2}{R_1}, \tag{37}$$

$$C_5 = C_1[24C_1^3\ln\frac{R_1}{R_2}\ln(R_1R_2) + 3C_1(13(-R_1^4 + R_2^4) + 12(R_1^4\ln R_1 - R_2^4\ln R_2))\left(\ln\frac{R_2}{R_1}\right)^2 +$$
$$+6C_1^2\left(-6C_1 + 8(R_1^2\ln R_1 - R_2^2\ln R_2) + 3(R_1^2 + R_2^2)\ln\frac{R_1}{R_2}\ln(R_1R_2)\right)\ln\frac{R_2}{R_1} +$$
$$+2(-13(R_1^6 - R_2^6) - 9R_1^2R_2^2C_1)\left(\ln\frac{R_2}{R_1}\right)^3 - 12(R_1^2 + R_2^2)(R_1^4 + R_2^4)\left(\ln\frac{R_2}{R_1}\right)^4], \tag{38}$$

$$C_6 = \left[6C_1(R_1 - R_2)^2\left(C_1 + (R_1^2 + R_2^2)\ln\frac{R_2}{R_1}\right)^3\ln\frac{R_2}{R_1}\right]^{-1}, \tag{39}$$

$$C_1(r) = ((r^2 - R_1^2)\ln\frac{R_2}{R_1} + C_1\ln\frac{r}{R_1})(16\ln\frac{R_2}{R_1})^{-1}, \tag{40}$$

$$C_2(r) = \frac{R_1}{4} + (R_1 + R_2)\left[8R_1R_2\left(\ln\frac{R_2}{R_1}\right)^2\right]^{-1}\left[C_1\ln\frac{R_1}{r} + R_2\left(R_1 - R_2 - 2R_1\ln\frac{r}{R_1}\right)\ln\frac{R_2}{R_1}\right], \tag{41}$$

$$C_3(r) = 54C_1^3\ln\frac{r}{R_1} + \left\{9C_1^2\left[6(r^2 - R_1^2) + \left(7(R_1^2 + R_2^2) + 4r^2\left(\ln\frac{r}{R_1} - 2\right)\right)\ln\frac{r}{R_1}\right] + \right.$$
$$+[C_1(-9(r^2(r^2 - 8R_1^2) + 7R_1^4) + 2(9r^2(r^2 - 4R_1^2) + 11(R_1^2(R_1^2 + R_2^2) +$$
$$\left. +R_2^4))\ln\frac{r}{R_1}\right) + 2(r^2 - R_1^2)(r^2(2r^2 - 7R_1^2) + 11R_1^4)\ln\frac{R_2}{R_1}\Big]\ln\frac{R_2}{R_1}\Big\}\ln\frac{R_2}{R_1}, \tag{42}$$

$$C_4(r) = \frac{1}{256}\left[C_1\left(C_1\ln\frac{R_2}{r} + (R_1^2 + R_2^2 - 2r^2)\ln\frac{R_2}{R_1}\right)\left(\ln\frac{R_2}{R_1}\right)^{-2}\ln\frac{r}{R_1} - (r^2 - R_1^2)^2\right], \tag{43}$$

$$C_5(r) = 36C_1^3\ln\frac{r}{R_1}\ln\frac{R_1}{R_2}\ln(R_1R_2) + 18C_1^2\left\{2(r^2 - R_1^2)\ln\frac{R_1}{R_2}\ln(R_1R_2) + \right.$$
$$\left. + \left[-3C_1 + 4(R_1^2\ln R_1 - R_2^2\ln R_2) + 2r^2\ln\frac{R_2}{R_1}\ln(R_1R_2)\right]\ln\frac{r}{R_1}\right\}\ln\frac{R_2}{R_1} -$$
$$9C_1^2\left[6(r^2 - R_1^2) + 3(R_1^2 + R_2^2)\ln\frac{r}{R_1} + 8R_1^2\ln R_1 + 4r^2 \cdot\right.$$

$$\left((-2+\ln r)\ln r-(\ln R_1)^2\right)\left]\left(\ln\frac{R_2}{R_1}\right)^2-\right.$$

$$C_1[-9(r^2-R_1^2)(r^2-3R_1^2-4R_2^2)+2(9r^4-18r^2(R_1^2+R_2^2)+$$

$$+11\,(R_1^4+R_1^2R_2^2+R_2^4)\Big)\ln\frac{r}{R_1}\Big]\left(\ln\frac{R_2}{R_1}\right)^3+2(R_1^2-r^2)(2r^4-7r^2R_1^2+11R_1^4)\left(\ln\frac{R_2}{R_1}\right)^4. \qquad (44)$$

Submitted 27.6.2024
Revised 12.8.2024.
Accepted 19.8.2024